NEW MAP OF ORIENTALE BASIN EJECTA AND COMPARISON OF EJECTED LOWLAND AND HIGHLAND MATERIAL. Z. R. Morse[1], G. R. Osinski[1, 2], and L. L. Tornabene[1], [1]Centre for Planetary Science and Exploration / Department of Earth Sciences, University of Western Ontario, 1151 Richmond Street, London Ontario, Canada, N6A 5B7, (zmorse@uwo.ca) [2]Department of Physics and Astronomy, University of Western Ontario, 1151 Richmond Street, London, Ontario, Canada, N6A 3K7.

Introduction: Orientale Basin is one of the youngest and best-preserved examples of a multi-ring impact basin in the Solar System [1]. Centered at 266.5º E, 19.5º N, Orientale is thought to have formed at the end of the Late Heavy Bombardment period approximately 3.8 billion years ago [2]. Orientale has a central depression that is ~950 km in diameter with three concentric rings; the Inner Rook Mountains, the Outer Rook Mountains, and Montes Cordillera [3, 4]. Several studies have used recent data obtained by the Lunar Reconnaissance Orbiter (LRO) and Gravity Recovery and Interior Laboratory (GRAIL) spacecraft to analyze the basin's mare fill, high gravitational anomaly, and map the interior of the basin [5, 6, 7]. Our study focuses on the impact ejecta deposits of Orientale. Known as the Hevelius Formation [1, 8], the blanket of ejecta material from Orientale extends from the base of the Cordillera ring over 1000 km across the lunar surface.

Previous Mapping. The only available maps of the Hevelius Formation are those produced by Moore et al. [1] and Scott et al. [9] in the 1970's using images obtained by the Lunar Orbiter IV and Zond 8 spacecraft. Our mapping effort benefits from new datasets of high-resolution images obtained by the Wide Angle Camera (WAC) and Narrow Angle Camera (NAC) onboard LRO. These images allowed us to redefine the facies boundaries established by the previous mapping efforts, as well as identify new facies, making our map the most accurate map [Fig. 1] of the Hevelius Formation yet produced.

Geologic Setting. The location of Orientale Basin is unique in that it straddles the dichotomy boundary between the nearside lunar lowlands and the far-side lunar highlands. This means that the material composing the ejecta blanket was excavated from depth from both of these distinct terrains

Methods: The ejecta blanket was primarily observed using a global mosaic of LRO-WAC images with a resolution of ~100 m/pixel [10]. In order to better define facies boundaries and individual facies morphology at a smaller scale LRO-NAC images were used with resolutions up to ~0.5 m/pixel [10]. These images were overlain on a digital elevation model derived from topography data obtained by the Lunar Orbiter Laser Altimeter (LOLA) which was sampled with 5 m laser spots spaced 25 m apart, providing a vertical resolution of 10 cm per sample point and a horizontal resolution of 1024 pixels per degree [11]. All GIS analysis was conducted using the JAVA Mission-planning and Analysis for Remote Sensing (JMARS) GIS suite [12].

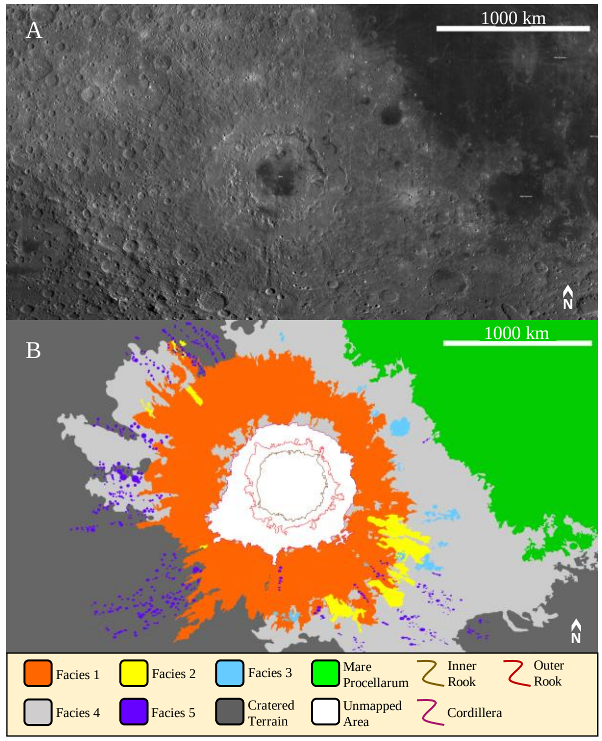

Figure 1 - A: *Orientale Basin in WAC Global Mosaic. Credit: NASA; LRO-WAC Mosaic*
B: *New Geologic Map of Basin Ejecta*

Results and Interpretations: Our mapping endeavor has resulted in the identification of 5 unique facies of ejecta material that are directly related to the Orientale impact event.

Facies 1. The first facies (orange) displays prominent radial ridges and extends from the base of the Cordillera range to ~400 to ~500 km outside of the ring. The radial ridges and troughs extend for the entire width of the facies and are often hundreds of kilometers from peak to valley. This facies extends radially in all directions, encircling the entire basin. We interpret this unit on our map as the ballistic ejecta excavated from the basin interior during the impact.

Facies 2. The second facies (yellow) also displays ridges, but these are often concentric to the basin rings. These ridges appear more like pressure ridges observed in surface lava flows [8, 13, 14]. These ridges indicate movement toward local topographic lows and around topographically high obstacles. This facies does not appear to be linked directly to the basin interior, but instead sits independently ~450 to ~600 km outside of the Cordillera ring. This facies appears to overlay the first facies (orange), and is most prominent in the southeastern portion of the ejecta blanket. Our observations show that this yellow unit also clearly exhibits flow-like textures consistent with melt-bearing ejecta materials [8, 13, 14]. We posit that these units were flows of melt that moved down slope in accordance with local topography, eventually cooling and solidifying in the shapes and positions observed today.

Facies 3. The third facies (blue) appears in isolated topographically low areas. These deposits have very flat surfaces and are dark in color. Again, there are several locations where this facies appears to overlay Facies 1. Deposits of Facies 3 also exist beyond the radial extent of Facies 1 in a number of places. This facies is observed in several locations in the eastern half of the ejecta blanket, but does not appear on the western half. Like Facies 2, the deposits comprising Facies 3 are interpreted to have also been molten ejecta that settled in topographic lows. However, unlike the flow morphology observed in Facies 2, the melt materials comprising Facies 3 completely filled in topographic lows and ponded evenly across equipotential surfaces.

Facies 4. The fourth (light gray) comprises low lying, rolling hills that has only been lightly modified by ejecta from Orientale basin. This hummocky topography does contain some small secondary impacts from the initial basin-forming event, but overall appears to be covered by only the finest ejecta particles. This unit is interpreted to be discontinuous ejecta composed of small blocks of ejected material.

Facies 5. The final facies (indigo) appears to be distinct chains of secondary impact craters. These chains extend radially from the basin center and can be observed nearly all the way around the basin. These chains usually extend from the distal reaches of the first radial facies, and continue on across the lunar surface for hundreds of kilometers. These crater chains are much more prominent in the western half of the basin ejecta. They are interpreted to be an extension of the radial ballistic ejecta, representing some of the larger ejecta blocks thrown out of the basin center.

Discussion and Conclusions: There are two main conclusions that can be drawn from these observations. First, the presence of melt flows and ponds overlying ballistic ejecta from the same impact event indicate that the impact melt was deposited after the ballistic ejecta in a later episode of ejecta emplacement. This type of multistage emplacement has been suggested around smaller simple and complex craters [14, 15], but to date, had not been observed around an impact basin. Our results provide evidence that a multistage emplacement model could be scaled up to include basin-sized impacts. Our second conclusion is that there are significant differences in surface morphology between the eastern and western halves of the Orientale ejecta blanket indicating compositional and rheological differences in the lunar lowland and highland terrains [Fig. 2].

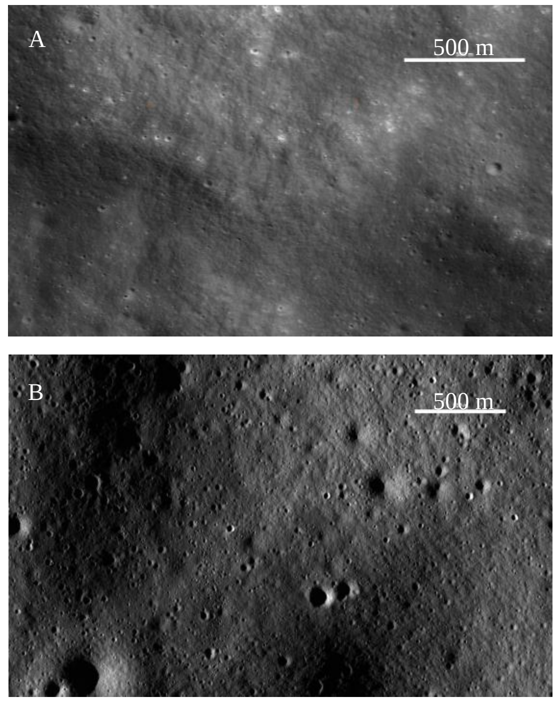

Figure 2 - A: *NAC Image of Smooth Eastern Radial Ejecta*
B: *NAC Image of Rough Western Radial Ejecta*
Credits: NASA; LRO-NAC

References: [1] Moore H. J. et al. (1974) 5th Lunar Conference, 1, 71–100. [2] Wetherill G. W. (1975) *LPSC VI*, 1539-1561. [3] McCauley J. F. (1977) *Physics of the Earth and Planetary Interiors*, 15, 220-250. [4] Hodges C. A. and Wilhelms D. E. (1978) *Icarus*, 34(2), 294-323. [5] Wieczorek M. A. et al. (2013) *Science*, 339(6120), 668-71. [6] Zuber M. T. et al. *Science*, 339(6120), 668-71. [7] Spudis P. D., Martin D. J. P., and Kramer G. (2014) *Journal of Geophysical Research: Planets*, 119(1), 19-29. [8] Hawke and Head (1977) *Impact and Explosion Cratering*, 815-841. [9] Scott D. H. et al. (1977) Geologic Map of the West Side of the Moon, USGS Map I-1034. [10] Robinson M. (2010) *Space Science Reviews*, 150, 81-124. [11] Chin G. et al. (2007) *Space Science Reviews*, 129(4), 391-419. [12] Christensen P. R. et al. (2009) American Geophysical Union Abstract #IN22A-06. [13] Bray V. J. et al. (2010) *Geophysical Research Letters*, 37, 1-5. [14] Denevi B. W. et al. (2012) *Icarus*, 219, 665-675. [15] Osinski et al. (2011) *Earth and Planetary Science Letters*, 310, 167–181.